CrossMark

Binder Jetting: A Novel NdFeB Bonded Magnet Fabrication Process

M. PARANS PARANTHAMAN,[1,7] CHRISTOPHER S. SHAFER,[1,2]
AMY M. ELLIOTT,[3] DEREK H. SIDDEL,[2,3] MICHAEL A. MCGUIRE,[4]
ROBERT M. SPRINGFIELD,[5] JOSH MARTIN,[5] ROBERT FREDETTE,[6]
and JOHN ORMEROD[6]

1.—Chemical Sciences Division, Oak Ridge National Laboratory, Oak Ridge, TN 37831, USA.
2.—The University of Tennessee, Knoxville, TN 37996, USA. 3.—Energy and Transportation
Science Division, Oak Ridge National Laboratory, Oak Ridge, TN 37831, USA. 4.—Materials
Science and Technology Division, Oak Ridge National Laboratory, Oak Ridge, TN 37831, USA.
5.—Tru-Design, LLC, Knoxville, TN 37938, USA. 6.—Magnet Applications, Inc., DuBoise,
PA 15801, USA. 7.—e-mail: paranthamanm@ornl.gov

The goal of this research is to fabricate near-net-shape isotropic $(Nd)_2Fe_{14}B$-based (NdFeB) bonded magnets using a three dimensional printing process to compete with conventional injection molding techniques used for bonded magnets. Additive manufacturing minimizes the waste of critical materials and allows for the creation of complex shapes and sizes. The binder jetting process works similarly to an inkjet printer. A print-head passes over a bed of NdFeB powder and deposits a polymer binding agent to bind the layer of particles together. The bound powder is then coated with another layer of powder, building the desired shape in successive layers of bonded powder. Upon completion, the green part and surrounding powders are placed in an oven at temperatures between 100°C and 150°C for 4–6 h to cure the binder. After curing, the excess powder can be brushed away to reveal the completed "green" part. Green magnet parts were then infiltrated with a clear urethane resin to achieve the measured density of the magnet of 3.47 g/cm^3 close to 46% relative to the NdFeB single crystal density of 7.6 g/cm^3. Magnetic measurements indicate that there is no degradation in the magnetic properties. This study provides a new pathway for preparing near-net-shape bonded magnets for various magnetic applications.

INTRODUCTION

Permanent magnets are used for many different applications including electromechanical machines such as motors, generators and electronic devices such as speakers, and hard disk drives.[1] Neodymium and dysprosium, used in $(Nd)_2Fe_{14}B$-based (NdFeB) magnets, were both reported as critical elements in the 2011 U.S. Department of Energy's Critical Materials Strategy Document with respect to importance to clean energy and supply risk.[2–6] Typical sintered manufacturing techniques waste magnetic material from the cutting, grinding, and machining steps of the shaping process or at the very minimum are limited in the geometric complexity that can be achieved. The complex geometries can be achieved using the current bonded magnet manufacturing techniques. However, tooling is necessary for printing new designs. Additive manufacturing (AM) is a unique method of fabrication that creates a complex shape from a computer-aided design (CAD) which requires little or no tooling and post-processing, thus reducing the amount of waste generated.[7] The main goal of this research is to develop an AM process to fabricate bonded magnets in complex geometries.

The bonded magnet fabrication process generally involves mixing magnet powders with a polymer (typically a thermoset, thermoplastic or elastomers) and produces various shapes and sizes of magnets through injection molding, calendaring, roll molding, compaction molding and extrusion molding. Materials and associated processes for bonded magnet fabrication have been reported in detail in the

literature.[8–16] It is desirable to maximize the magnetic particle loading to achieve high volumetric densities and hence increased magnetic properties for the bonded magnet. In addition, high mechanical flexibility introduced by the polymer allows for fabrication of various geometries thus providing versatility in design. Many different methods exist to produce geometries in a layer-wise fashion including thermoplastic extrusion through a heated nozzle, melting of a powder feedstock via an electron beam, and deposition of a photopolymer via inkjet.[17] Due to the versatility of the process, binder jetting AM is utilized and evaluated in this research for feasibility and performance to fabricate near-net-shape NdFeB bonded magnets. Binder jetting AM uses an inkjet print-head to selectively deposit a binder or binding agent to a bed of powdered material, binding the powder together into the desired shape.[7,18] The resulting printed "green" part can be either strong or weak depending on the properties of the binder. Post-processing of green parts includes sintering, infiltration, or coating. The binder jetting process has been successfully used to demonstrate complex shapes of functional materials.[7,18] Here, we report our successful fabrication of NdFeB bonded magnets using a binder jetting process and the resulting magnet properties.

SHAPING NdFeB POWDERS VIA BINDER JETTING

The binder jetting AM process involves a powder bed for the build area, a roller, an inkjet print-head, and either a powder hopper or feed bin which supplies the powder. The process starts by dropping the build volume by the desired layer thickness and spreading a thin layer of powder over the build area with the roller. The print-head then passes over the build area and selectively deposits binder into the 2D cross-sectional shape of the current layer. The build volume drops again, more powder is spread, and the process continues until all layers of the part are completed. The first step in three dimensional printing bonded magnets using the ExOne® binder-jet printer is creating a CAD model of the desired shape. Step two involves exporting the CAD model as a.stl file which divides the model into triangles that the printer software divides into layers based on the triangles. Here, isotropic NdFeB magnet powder particles (Magnequench) are spread evenly over the feed and build sides of the print bed and printing can begin. The build side, where the binder is deposited, drops by one layer thickness and the feed side, containing powder for subsequent layers, rises by the same distance. The print bed then moves under a heat lamp to set the bound powder and is subsequently covered in a new layer of powder by moving under the roller.

Upon printing completion, the entire build side of the print bed was removed and placed in an oven for curing of the binder. Curing temperatures ranged from 100°C to 150°C for 4–6 h; higher temperatures require less time to cure the binder. After cooling, the loose powder around the now cured and bound powder geometry can be brushed away revealing the bonded magnet. The unbound powder surrounding the printed geometry does not degrade during post-processing and can be used again for later prints. The magnet in this form is referred to as a "green" part, and it is brittle but still strong enough to be handled for post-processing. Post-processing of the green parts is necessary to improve the mechanical properties of the printed magnets. For post-processing magnetic materials, the primary challenge is to reduce the post processing conditions to temperatures below 300°C in order to minimize the loss of magnetic properties including coercivity and energy products. The specific details of the experiments will be discussed in the next section.

EXPERIMENTAL

A resin-coated MQP-B-20173-070 (referred to as MQP) isotropic NdFeB magnetic powder feedstock with an average diameter of around 70 μm was used for this study. Binder jet printing was performed with an ExOne X1-Lab printer. For this system, the packing density of the powder system as well as the desired saturation with the binder must be specified. With these two values, the printer can select a drop spacing that will produce the desired binder concentration in the printed regions. The following print settings were used with the magnetic powder in the binder jetting process: 0.2 mm layer thickness; 60% powder packing rate; 70% desired binder saturation; 0.5 (initial)–2.0 mm/s spread speed; and 25–40 s drying time between each coat. Because coarser
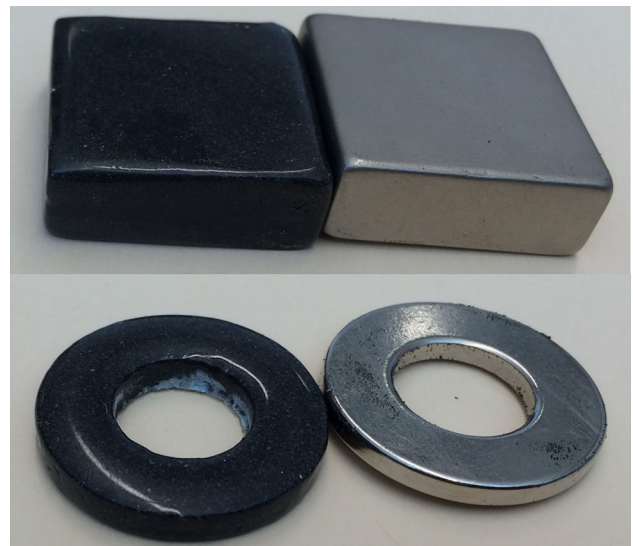

Fig. 1. Images of 1" × 1" square (2.54 × 2.54 cm) and 1" (2.54 cm) ring near-net-shape binder jet magnets after a clear polyurethane coat compared with nickel-coated commercially sintered NdFeB magnets.

powders flow more easily, the main challenge for printing the coarse magnetic powder was determining a spreading speed that would not dislodge the printed regions from the loose powder bed. Magnets with 25.4 mm × 25.4 mm × 9.525 mm thick square geometry and 25.4-mm-diameter OD × 2.54-mm-thick ring geometry were printed.

After printing, the printed parts were heated in an oven to cure the binder with the optimum curing temperatures ranging from 100°C to 150°C for 4–6 h. The surfaces of the printed magnets were generally porous and rough due to the coarseness of the powder feedstock. In order to improve the mechanical strength and also improve the surface
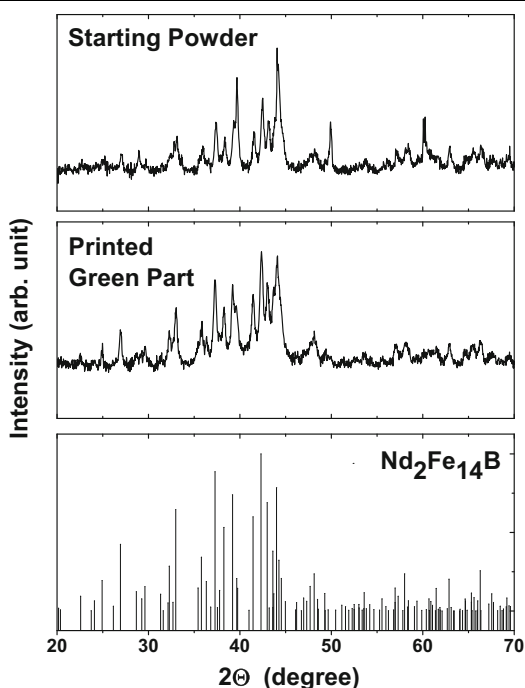

Fig. 2. XRD patterns of as-received MQP powders (top) and binder jet printed magnet part (center). The vertical lines indicate the peak positions for $Nd_2Fe_{14}B$ phase (bottom).

quality, binder jet magnets were dip-coated in Axalta's Standox 15–60 + production clear urethane resin. Standox 15–25 hardener was used for these experiments. The urethane resin system with a low viscosity was chosen with the expectation that it would fully saturate the magnets. The green magnets were placed in a wire fixture and immersed for approximately 5 min to permit the resin to infiltrate the porous magnet structure. The immersion process was repeated until the magnet no longer absorbed resin and the surface was fully coated. Thirty minutes was allowed between the immersions while the magnet remained in the dipping fixture suspended in room temperature. Contact points were touched-up with resin followed by wet sanding and buffing to remove any marks from the fixture.

PANalytical X'Pert powder diffractometer with Cu kα radiation (λ = 1.54056 Å) was used to study the phase fractions of various phases in the binder jetting magnet and compared with the as-received powders. Sections were then prepared for metallographic analysis and polished using standard metallographic techniques. Microstructure analysis of the deposit was then performed using a HITACHI 3400S SEM operated at an accelerating voltage of 20 kV. Magnetization data was collected with a Quantum Design MPMS-5 SQUID magnetometer. Hysteresis loops of the binder jet printed ring and square magnets were collected with AMH-500 (Laboratorio Elettrofisico) automatic hysteresisgraph with 100-mm pole pieces.

RESULTS AND DISCUSSION

Figure 1 shows a comparison between the binder jet magnets and the sintered NdFeB magnets. As shown in Fig. 1, near-net-shape magnets were successfully printed. Phase composition, microstructure, and magnetic flux were measured before and after printing to determine the effect of binder jetting on these properties. Figure 2a and b present the XRD patterns of the MQP powder before and after
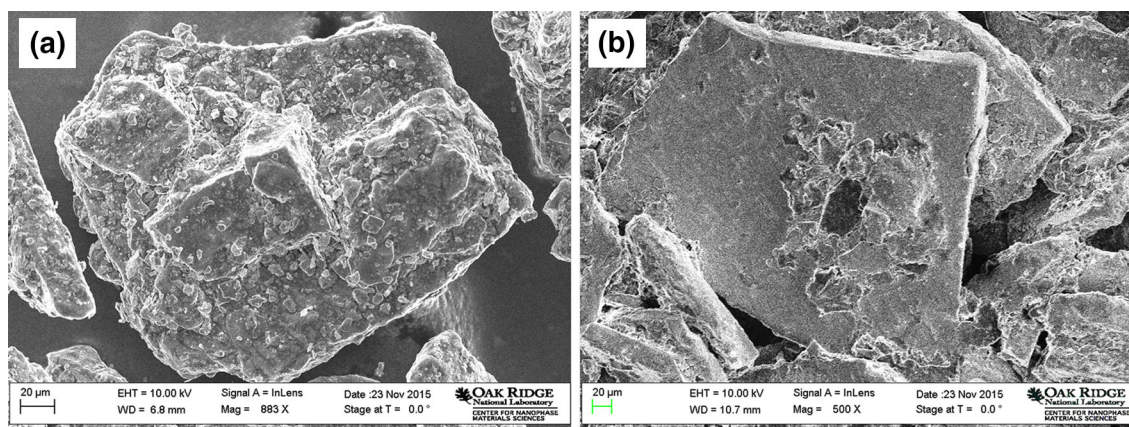

Fig. 3. SEM images of (a) as-received commercial MQP powders, and (b) binder jet printed magnet part.

printing, respectively. With the presence of similar $Nd_2Fe_{14}B$ phases in these two figures, it can be concluded that the printing of the powder did not cause any major change in the phase fraction of the magnetic powder. Similarly, SEM images of the powder before and after printing shown in Fig. 3a and b reveal there is no change in the morphology. About 46 vol.% (equivalent to 85 wt.%) magnet powders were loaded into the binder jet magnet samples. The magnetic hysteresis loops for the printed green parts are plotted in Fig. 4. The intrinsic coercivity of the green body is found to be 716.2 kA/m from this data. This can be compared to the reference data for the starting powder (MQP-B-20173-070) that states intrinsic coercivity of 692.3–748.0 kA/m. This demonstrates that the coercivity of the powder, which is very sensitive to the microstructure, is not degraded by the processing methods employed. The measured density of the whole binder jet square

magnet piece was 3.47 g/cm^3. This corresponds to 46 vol.% of the NdFeB density of 7.6 g/cm^3. The field dependence flux densities for the whole binder jet ring and square magnet pieces are shown in Fig. 5, which indicates that the remanence of the binder jet magnet samples is about 0.3 T. This compares to the remanence values of 0.5 T and 0.65 T for standard production injection molded and compression bonded isotropic NdFeB magnets. The volume fraction of NdFeB powders in production injection molded and compression bonded NdFeB magnets is typically 0.65 and 0.80, respectively. Based on these values, one can estimate that the volume fraction of NdFeB powder in the binder jet magnets is approximately 0.45. Clearly, one of the challenges in utilizing the binder jet process to fabricate competitive magnetic performance will be the increase in volume fraction of the NdFeB powder in the magnet body. Hence, a focus of our future research will be to increase the volumetric densities of the printed magnets using bimodal distribution of particle sizes with a micron or submicron size and 70 μm-sized particles.

CONCLUSION

This study presents a novel method to fabricate near-net-shape NdFeB bonded magnets through a binder jetting AM process. Binder jet magnets with the measured density of nearly 46% were achieved. Thus, a long-term challenge for bonded magnets is to further densify using bimodal starting particles and/or infiltrate nanoparticles/micron-sized particles into the green part. The permanent magnetic properties of the printed parts were found to be consistent with those of the powder used, with no indication of processing-induced degradation. Further investigation to increase magnetic particle
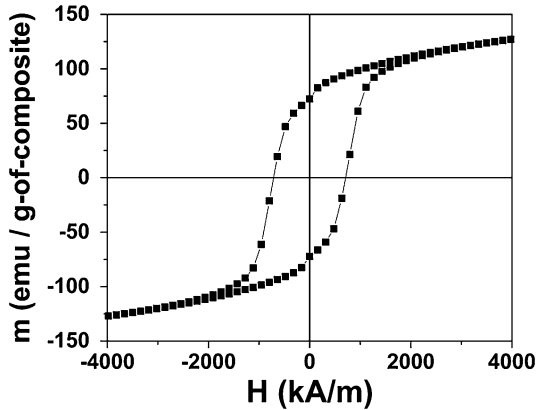

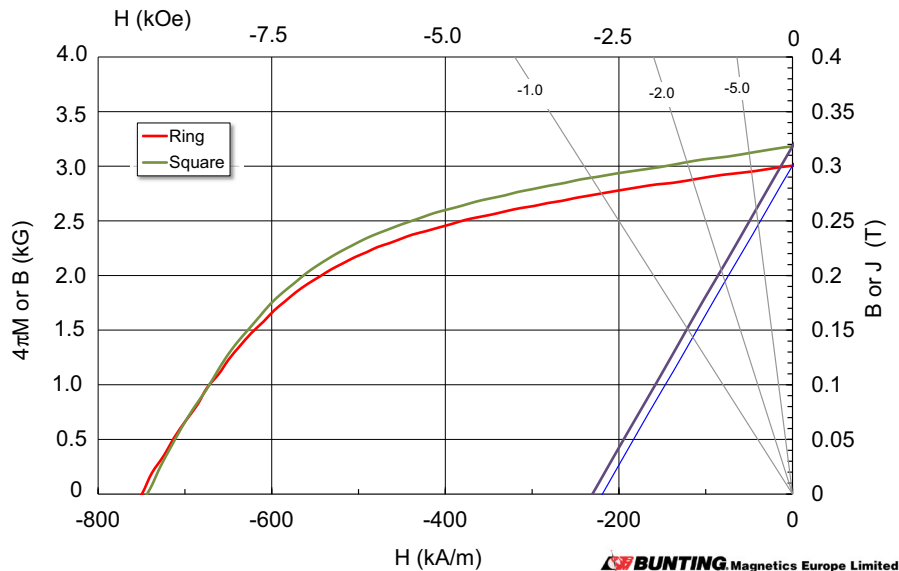Fig. 4. Hysteresis loops of binder jet printed MQP magnet material.

Fig. 5. Hysteresis loops of the binder jet printed ring and square magnets.

loading and optimize post-processing conditions using suitable binders is needed to fabricate high-performance bonded magnets in the future.

REFERENCES

1. K.J. Strnat, *Proceedings of the IEEE* 78, 923 (1990).
2. D. Bauer, D. Diamond, J. Li, D. Sandalow, P. Telleen, and B. Wanner, *USDOE Critical Materials Strategy*, 1 (2010).
3. U. S. Department of Energy—Critical Materials Strategy (2011) December Report.
4. S. Hirosawa, Y. Matsuura, H. Yamamoto, S. Fujimura, and M. Sagawa, *J. Appl. Phys.* 59, 873 (1986).
5. E.B. Boltich, E. Oswald, M.Q. Huang, S. Hirosawa, W.E. Wallace, and E. Burzo, *J. Appl. Phys.* 57, 4106 (1985).
6. H. Ucar, I.C. Nlebedim, M.P. Paranthaman, and R.W. McCallum, *J. Appl. Phys.* 116, 233901 (2014).
7. S.M. Gaytan, M.A. Cadena, H. Karim, D. Delfin, Y. Lin, D. Espalin, E. MacDonald, and R.B. Wicker, *Ceram. Int.* 41, 6610 (2015).
8. J. Ormerod and S. Constantinides, *J. Appl. Phys.* 81, 4816 (1997).
9. N. Hamada, C. Mishima, H. Mitarai, and Y. Honkura, *IEEE Trans. Magn.* 39, 2953 (2003).
10. Hamada, K. Noguchi, C. Mishima, and Y. Honkura, "Development of Anisotropic Bonded Magnet with Heat Resistance", *Magnetic Conference, Intermag Asia 2005, Digests of the IEEE International*, pp. 941–942 (2005).
11. J.J. Croat, *J. Appl. Phys.* 81, 4804 (1997).
12. S. Sugimoto, *J. Phys. D Appl. Phys.* 44, 064001 (2011).
13. D. Brown, B.M. Ma, and Z. Chen, *J. Mag. Mater.* 248, 432 (2002).
14. D.N. Brown, Z. Wu, F. He, D.J. Miller, and J.W. Herchenroeder, *J. Phys. Cond. Mat.* 26, 064202 (2014).
15. N. Hamada, K. Noguchi, C. Mishima, and Y. Honkura, *IEEE Trans. Magn.* 41, 3847 (2005).
16. D.N. Brown, Z. Chen, P. Guschl, and P. Campbell, *J. Mag. Mater.* 303, 371 (2006).
17. C.B. Williams, F. Mistree, and D.W. Rosen, *J. Mech. Des.* 133, 121002 (2011).
18. G. Manogharan, M. Kioko, and C. Linkous, *JOM* 67, 660 (2015).